Finite Element Modeling of Pressure Profile Around a Particle as in a Heterogeneous Nucleation Site

Lilac Cuiling Wang, Siu N. Leung Markus Bussmann and Chul B. Park

Department of Mechanical and Industrial Engineering, University of Toronto
Toronto, ON, M5S 3G8, Canada

Email: *lilac@mie.utoronto.ca*

ABSTRACT

In the polymer foaming process, pressure is a critical parameter that affects the degree of supersaturation within a polymer-gas solution. In most previous studies on cell nucleation, a uniform pressure throughout the solution was assumed. Although this assumption may be acceptable when no additives have been added, its validity is questionable when nucleating agents (talc, solid clay or mineral oil) are present. The discontinuity at the interface between the additives and surrounding material is a potential heterogeneous nucleation site, and so the pressure field around additive particles will be different from the bulk. In light of this, this paper presents a numerical analysis to investigate the pressure profile around cell nucleating agents. An interface tracking method is used so that the multiple phases are treated as a single-phase. The arbitrary Lagrangian-Eulerian (ALE) formulation is applied to describe the interface between the polymer melt mixture and the additives. The semi-torsional spring analogy method is used to describe the movement of the mesh as the additive particles move (or deform). Several cases are studied, and factors that affect pressure distribution are investigated. Such an investigation is expected to provide new information about the underlying mechanism that promotes cell nucleation in the presence of heterogeneous nucleating agents.

1. INTRODUCTION

Nucleating agents have long been employed in polymeric foaming processes to promote cell nucleation in order to increase cell density, reduce cell size, and improve cell uniformity. Using the classical thermodynamics, it has been proven that the presence of heterogeneous nucleating sites of various shapes will help to reduce the free energy barrier to initiate cell nucleation [1-4], and thereby aid in generating more cells. This was the basis of various theoretical studies [5-10] of polymeric foaming processes over the past few decades. In these studies, researchers used the system pressure in the foaming equipment to approximate the pressure inside the polymer-gas solution during foaming processes, but this assumption ignored the local pressure fluctuation. It is believed that during a polymeric foaming process, the local movement of the polymer-gas solution caused by the expansion of a nucleated bubble will induce a stress field within the polymer matrix. The discontinuity between the nucleating agent and the surrounding polymer may lead to a local pressure field that is different from the bulk.

According to the classical nucleation theory [11-12], both the free energy barrier for heterogeneous nucleation (W_{het}) and the critical radius for bubble nucleation (R_{cr}) depend on the local pressure in the polymer matrix:

$$W_{het} = \frac{16\pi\gamma_{lg}^{3} F(\theta_c, \beta)}{3\left(P_{bub,cr} - P_{sys}\right)^2} \quad (1)$$

$$R_{cr} = \frac{2\gamma_{lg}}{P_{bub,cr} - P_{sys}} \quad (2)$$

where γ_{lg} is the surface tension at the polymer-gas interface; $P_{bub,cr}$ is the pressure in a critical bubble; and P_{sys} is the local pressure in the polymer matrix; F is the ratio of the volume of the heterogeneously nucleated bubble to the volume of a spherical bubble having the same radius; parameters θ_c and β are related to interfacial properties of a particle and the geometry of the particle respectively.

While pioneering studies [13-15] provide some qualitative insights into stress-induced cell nucleation, this paper is the first attempt to study the local stress field around heterogeneous nucleating sites during polymeric foaming process. As a result,

it aims to provide new insights to understand cell nucleation phenomena in the presence of heterogeneous nucleating agents. The results are from a numerical model that model pressure changes in response to given conditions. In the following sections, a mathematical model based on the physical laws and assumptions is introduced; the numerical algorithm for solving the pressure field around a heterogeneous nucleating site is explained; and finally, several cases are studied and the simulation results are presented.

2. METHODOLOGY

2.1 Heterogeneous Nucleation Site and Solid Particle Dynamics

A nucleated bubble with a solid clay particle in close vicinity in a 3D finite volume of polymer gas solution is considered as a model of a nucleation site. A schematic graph is illustrated in Figure 1. The dynamics of a solid particle in a polymer gas solution is complicated due to the nucleation process induced flow filed and the small size of the particle. It is speculated that, with the existence of solid particles in the polymer matrix, the shear/extensional flow in the expansion of nucleated bubbles near these particles would generate biaxial stretching or shear action near these heterogeneous nucleating sites, and thereby generate shear/extensional fields within these local regions.

When a nucleated bubble is expanding, the biaxial stretching within the cell wall will result in an extensional flow around a solid clay particle in vicinity. Consequently, the solid clays tend to orient along the cell walls whereas they disperse randomly in the central area of the junction [16]. Since the extensional force is a function of the distance between the clay and the bubble, it will impel the clay to move, together with the melt, towards the expanded bubble. In other words, the overall movement of the clay will be identical to the net movement of the melt being caused by the expanding bubble. Also, the asymmetrically distributed expanding bubbles around the clay may cause the clay tumbling or turning due to the fact that the clay may have a large L/D ratio. The tumbling or turning also generates local shear fields around the clay, although overall the clay is moving apart from the expending bubble with the melt. The extensional flow being induced by the biaxial stretching generates a local pressure field around the side surface of the solid clay particle; such local pressure field may significantly promote cell nucleation.

2.2 Interface Tracking Method

The mixture of polymer melt and blowing agent can be considered to be a single-phase fluid. However, the presence of *0.5-5wt%* solid clay makes the mixture a two-phase (liquid and solid) material. In this study, an interface tracking method is used, and yet the different phases are treated as a single-phase, and so a single set of governing equations are solved for the whole computational domain. The interface tracking method has been widely used [17-19] in numerical modeling to treat a multiphase flow as a single phase. It is a suitable method for this study because the weight percent of the clay is small, and only a nano-scale site is considered. The modeling is carried out for the mixture of polymer melt, and the interface between the polymer melt and the solid clay is tracked explicitly by an unstructured adaptive mesh.

2.3 Conservation Laws

The mixture of polymer melt and blowing agent consisting of nucleating agent particles is assumed to be a single-phase mixture, and the flow is assumed incompressible and steady state, if the particle does not move; the flow is assumed to be unsteady if the particle moves with the flow field or deforms due to the shear stress of the flow. The flow complies with conservation laws for mass and momentum, which are in the form of a set of partial differential equations:

$$\nabla \cdot u = 0 \tag{3}$$

$$\rho \frac{DU}{Dt} = \nabla \bullet \sigma + f \tag{4}$$

u is the velocity vector, σ is the stress tensor, ρ is fluid density, and f is an external force term. The stress tensor is required to obey the constitutive equations:

$$\sigma = -PI + \tau \tag{5}$$

and

$$\tau = 2\mu(\dot{\gamma})d \tag{6}$$

where P is the fluid pressure, I is the identity tensor, μ is the dynamic viscosity, and d is the rate-of deformation tensor given by:

$$d = \frac{1}{2}\left[\left(\nabla u\right) + \left(\nabla u\right)^T\right] \tag{7}$$

where $\dot{\gamma}$ is the local shear rate defined by

$$\dot{\gamma} = \sqrt{2tr(d \bullet d)} \tag{8}$$

The polymer melt is modeled as a purely viscous fluid, where the shear rate ($\dot{\gamma}$) dependent viscosity of the melt is described by a power-law model:

$$\mu(\dot{\gamma}) = m(\dot{\gamma})^{n-1} \tag{9}$$

where m is the consistency index and n is the power-law index. In this case, an isothermal condition was assumed.

2.4 ALE Formulation

The arbitrary Lagrangian-Eulerian (ALE) formulation is applied to describe the interface between the polymer melt mixture and the solid clay or mineral oil. The ALE formulation is a generalized kinematic description that allows arbitrary mesh movement with the mesh velocity decoupled from the fluid velocity. The governing equations (3) and (4) are non-dimensionalized by introducing a non-dimensional Reynolds number $\mathrm{Re} = UL/\mu$. L is a flow characteristic length, U is a characteristic velocity and μ is the dynamic viscosity. The non-dimensional form of the governing equations (neglecting the external term) after the ALE formulation is applied, is:

$$\nabla \cdot u = 0 \tag{10}$$

$$\alpha^2 \frac{\partial u}{\partial t} + \mathrm{Re}(u - u^G)\nabla u = -\mathrm{Re}_1 \nabla P + \nabla \bullet [\mu \bullet (\nabla u) + (\nabla u)^T] \tag{11}$$

where u^G is the mesh velocity. If the nucleating clay does not deform or is not moving with the flow, $u^G = 0$; otherwise, a moving boundary case is considered. For molten polymer flow, the Reynolds number is very small, usually in the range of $10^{-4} - 10^{-2}$.

2.5 Numerical Algorithm

The governing equations (10) and (11) are spatially discretized using a Galerkin finite element approach in conjunction with P2-P1 tetrahedral Taylor-Hood elements. The unknown velocity and pressure fields are expressed in terms of the shape functions ϕ_j and ψ_j and the nodal velocity and pressure values u_j and p_j:

$$u = \sum_{j=1}^{N} u_j \varphi_j \tag{12}$$

$$p = \sum_{j=1}^{N_p} p_j \psi_j \tag{13}$$

where there are $N = 10$ degrees of freedom for velocity (in each co-ordinate direction) and temperature, and $N_p = 4$ degrees of freedom for pressure. Following a Galerkin spatial discretization, the governing equations are written in semi-discrete form as:

$$[M]\frac{d\{u\}}{dt} + ([N] - [N^G]) + [S]\{u\} + [L]^T\{p\} = \int_\Gamma (-pn + \frac{\partial u}{\partial n})\, dS \tag{14}$$

$$[L]\{u\} = 0 \tag{15}$$

where $\{u\}$ and $\{p\}$ are the vectors of nodal velocity and pressure. $[M]$, $[S]$ and $[L]$ are elemental matrices, S is the boundary of the elemental volume, and n is a normal vector.

2.6 Mesh Deformation

In modeling flow problems with moving boundaries, a technique needs to be applied to update the mesh when the domain deforms. A widely used approach is the spring analogy method, in which the edges of the mesh elements are considered to be fictitious springs. In this work, the semi-torsional spring analogy method is used to describe the movement of the mesh as the clay or mineral oil droplet moves. The semi-torsional spring analogy is derived from the lineal spring analogy and the torsional spring analogy by defining the stiffness of an edge (edge *i-j*) of an element as the sum of its lineal stiffness and its semi-torsional stiffness:

$$k_{ij} = k_{ij}^{\ lineal} + k_{ij}^{\ semi-torsional} \tag{16}$$

where $k_{ij}^{\ lineal}$ can be defined by the coordinates of the two nodes connected by an edge, and $k_{ij}^{\ semi-torsional}$ is defined as:

$$k_{ij}^{\ semi-torsional} = \sum_{m=1}^{NE_{ij}} \frac{1}{\sin^2 \theta_m^{\ ij}} \tag{17}$$

where NE_{ij} is the number of elements sharing edge *i-j,* and $\theta_m^{\ ij}$ is the facing angle, defined as the angle that faces the edge *i-j* on the *m*th element attached to the edge. The mesh-updating algorithm is implemented in a FEM code [20] for solving the 3D incompressible Navier-Stokes equations in an ALE formulation. The implementation was validated using flows with moving boundaries for simple cases.

3. RESULTS AND DISCUSSION

The numerical modeling is carried out for several cases. First, a solid rectangular plate, which can represent a particle or a group of particles of the nucleating agent (e.g., talc) in a polymer melt mixture, is considered. The plate may stick to a spot during foaming, when it is a group of particles; or move with the mixture flow, if it is a nano-scale particle. The movement can also be multiplex: it can simply move in the flow direction, or spin due to shearing. Some results of these cases are presented, to illustrate how pressure changes around the plate. Finally, numerical simulations were carried out for cases involving a mineral ball, as it deforms when the polymer melt mixture is squeezed. A summary of all the cases studied is listed in Table 1.

3.1 Geometry of the Nucleating Site and Simulation Parameters

A 3D rectangular plate or of a sphere is considered to be the geometry for cases studied. The rectangular plate and the sphere represents a solid nucleating clay and the mineral droplet submerged in the mixture of the polymer melt and blowing agent respectively. Figure 1 shows the numerical volume, a big sphere, with a bubble and solid plate inside. Figure 2 illustrates a solid clay in a biaxial stretching field. Figure 3 shows the spatial discretization, which is the finite element mesh for the geometry of a mineral ball in a melt.

The material considered in this study is WB130HMS polypropylene (PP) with 2wt% and 4wt% CO_2. An isothermal condition was assumed. A summary of material data used for the calculations, and the operating conditions considered, are listed in Table 2.

3.2 Rectangular Particle in a Polymer-Gas Mixture

Consider a solid plate that is moving as a nucleated bubble is expanding, Figure 1. The bubble is expanding at a given expanding rate, and the solid plate is impelled to move with the melt that is expanding radially outward from the bubble surface. The result of the flow field in vector form is show in Figure 4, and shows the radial motion of the flow field. The pressure profile along the vertical line as in Figure 4 is plotted for different time steps, Figure 5. The result indicates that, the pressure field around the solid plate is different from the system especially at the top and bottom of the clay. Negative pressure presents at the bottom of the clay which implies that a potential nucleation site around this area. Although the local pressure field differs from the system pressure, the overall pressure change is not significant as only a few tens Pas difference presents.

3.3 Solid Plate in a Biaxial Stretching Flow Field

First, consider a solid plate that is motionless in stretching field caused by the bubble expanding. This is a case when a solid particle has been oriented at some where in the melt. The simulation result of the pressure profile is shown in Figure 6, and indicates that a) the pressure around the solid plate is significantly different from that of the mixture; b) in the flow direction, there are extreme values of pressure at the top and the bottom of the plate; c) the pressure values at the top of the plate are negative. The negative pressure values around a solid particle are beneficial to cell nucleation because they will promote supersaturation; the pressure was plotted along the line AA in Figure 6 and the effect of the gas content is shown in Figure 7. Figure 7 indicates that, as the gas content increases, the pressure difference is smaller than the case with lower gas content. When more gas is added to the polymer solution, viscosity decreases and the shear effect decreases. Therefore, lower gas content is more favorite to nucleation. Figure 8 illustrates the effect of the distance between the solid clay and the bubble, and implies that when the bubble is more close to a plate, it would be beneficial to cell nucleation.

Second, consider a solid plate spinning in a shear flow about a fixed corner. A schematic is shown in Figure 9. The pressure profile along the line BB (Figure 10) was plotted against time. At the beginning, when the plate starts to spin, the pressure around the particle is high, but then the pressure approaches a constant value that the pressure is still higher than that of the mixture. Moreover, the pressure profile is higher than the case when the plate is immovable (Figure 5). This may due to the effect of shear on the plate.

3.4 Deforming Spherical Particle in a Polymer-Gas Mixture

A sphere or a droplet in a mixture of polymer melt is another case considered. The sphere is assumed a mineral oil droplet that can be deformed. The simulation was carried out for the case of a mineral oil droplet when the polymer mixture is squeezed. The pressure profile is shown in Figure 11. The surface stress on a squeezed sphere can be calculated.

When the spherical droplet is deformed, the stress changes at the surface of the droplet with a symmetric stress distribution at the top and the bottom of the sphere.

4 SUMMARY

Pressure is an important parameter that affects cell nucleation. The presence of cell nucleating agents that promote cell nucleation creates discontinuities in the foaming mixture. Numerical simulations of the pressure profiles around nucleating sites in a mixture of polymer melt and blowing agent have been carried out. The pressure profile around nucleating agents can vary significantly from the surrounding. Area where involves negative pressure distribution can induce cell propagation and the cell nucleation rate can be high. Nucleating site that is involved in stretching will significantly promote heterogeneous nucleation. Finally, a deformed particle in a mixture induces a change of the nearby stress and pressure fields, which is also beneficial to cell nucleation.

REFERENCES

[1] J.H. Han, and C.D. Han, *J. Polym. Sci.*, 28, 743 **(**1990).
[2] D. Turnbull, and B. Vonnegut, *Ind. Eng. Chem.*, 44, 1292 (1952).
[3] N.H. Fletcher, *J. Chem. Phys.*, 29, 572 (1958).
[4] N.H. Fletcher, *J. Chem. Phys.*, 31, 1136 (1959).
[5] R. Cole, *Adv. Heat Trans.*, 10, 85 (1974).
[6] J.G. Lee, and R.W. Flumerfelt, *J. Coll. Int. Sci.*, 184, 335 (1996).
[7] M.A. Shafi, K. Joshi, and R.W. Flumerfelt, *Chem. Eng. Sci.*, 52, 635 (1997).
[8] K. Joshi, J.G. Lee, M. Shafi, and R.W. Flumerfelt, *J. App. Polym. Sci.*, 67, 1353 (1998).
[9] M. Shimoda, I. Tsujimura, M. Tanigaki, and M. Ohshima, *J. Cellu. Plast.*, 3**7**, 517 (2001).
[10] D. Mao, J.R. Edwards, and A. Harvey, *Chem. Eng. Sci.*, 61, 1836 (2006).
[11] J.W. Gibbs, *The Scientific Papers of J. Willard Gibbs, Vol. 1*; Dover: New York, 337 (1961)..
[12] M. Blander, and J. L. Katz, *AIChE J*, 21, 833 (1975).
[13] S.T. Lee, *Polym. Eng. Sci.*, 33, 418 (1993).
[14] L. Chen, H. Sheth, and X. Wang, *J. Celul. Plast.*, 37, 353 (2001).
[15] C.Y. Gao, N.Q. Zhou, X.F. Peng, and P. Zhang, *Polym. Plast. Tech. Eng.*, 45, 1025 (2006).
[16] M. Okamoto, P.H. Nam, P. Maiti, T. Kptaka, N. Hasegawa, and A. Usuki, *Nano. Lett.*, **1**, 295 (2001).
[17] M. Sussman, E. Fatemi, *SIAM J. Sci Comp,* vol. 20, pp. 1165-1191 (1999).
[18] D. Lakehal, M. Meier and M. Fulgosi, *Int. J. of Heat and Fluid Flow*, 23, pp. 242–257 (2002).
[19] S.O. Unverdi, G. Tryggvason, *J. Comp Phys*, vol. 100, no. 1, p. 25-37 (1992).
[20] P. Minev and C. Ethier, *Comp Meth* Appl Mech *Eng* 192:1281–1298 (2003).

Table 1. Cases Studied

Cases	**Case I**	**Case II**	**Case III**
Geometry	A plate and a bubble in a sphere volume	A plate in a biaxial stretching field	A mineral ball in a volume
Expansion rate (Stretching Rate) dR/dt	$5\times10^{-5} m/s$	$5\times10^{-5} m/s$	$5\times10^{-5} m$
Distance: *ds*	5 μm	5/10/ 40 μm	-
Boundary Movement	Move with the melt /Spin	Fixed	moving
Deformation	No	No	squeeze

Table 2. Material data and operating conditions

Parameters	**Values**
Density (*g/ml*)	0.910
CO_2 Content (*wt%*)	2.0
Power-Law Index (*n*)	0.4
Power-Law Consistency ($pa \bullet s^n$)	5100
Reynolds Number (*Re*)	1.0×10^{-4}
Flow-Rate (*g/s*)	20 /0.002
Melt Temperature (*T*)	190

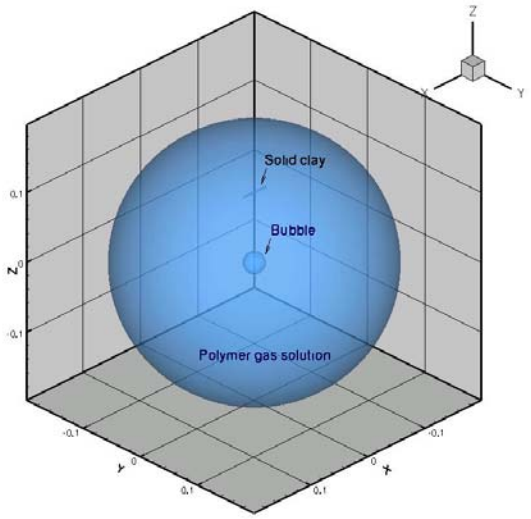

Figure 1. 3D numerical volume with a sphere bubble and rectangular clay submerged in a polymer-gas flow

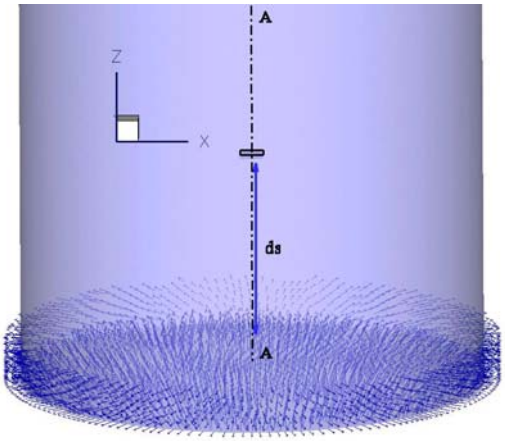

Figure 2. 3D numerical volume with a rectangular clay in a polymer-gas solution with a biaxial stretching field

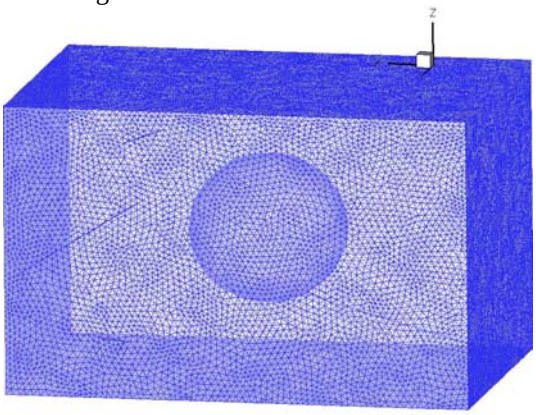

Figure 3. 3D Mesh for the geometry of the polymer gas solution with a mineral ball inside

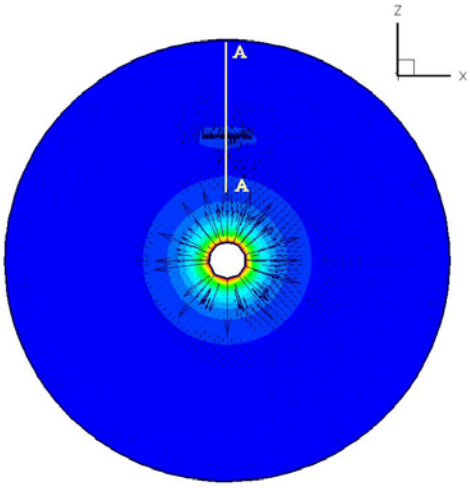

Figure 4. Velocity vector as the bubble grows

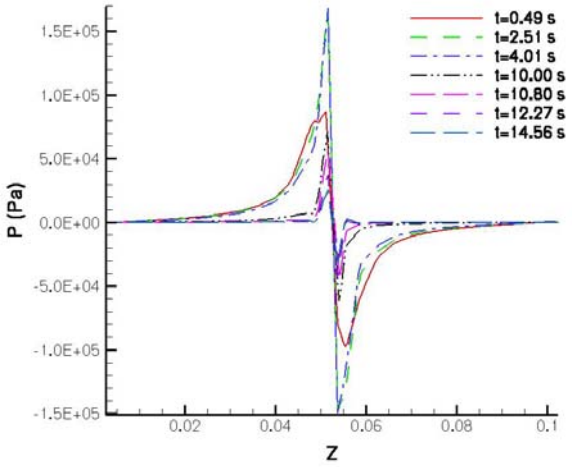

Figure 5. Pressure profile along line AA in Figure 4

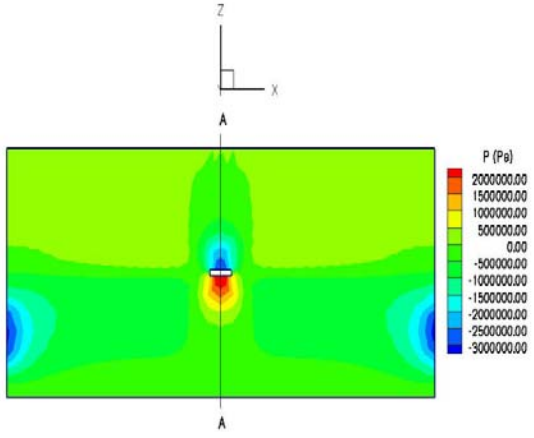

Figure 6. Pressure contour for case II when ds=0.0005mm

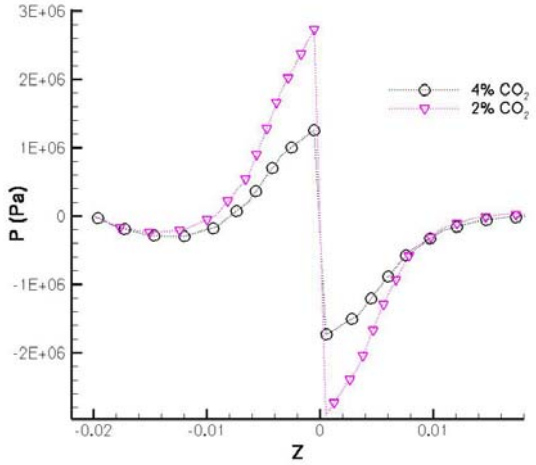

Figure 7. Pressure profile along line AA as in Figure 6; the effect of gas content

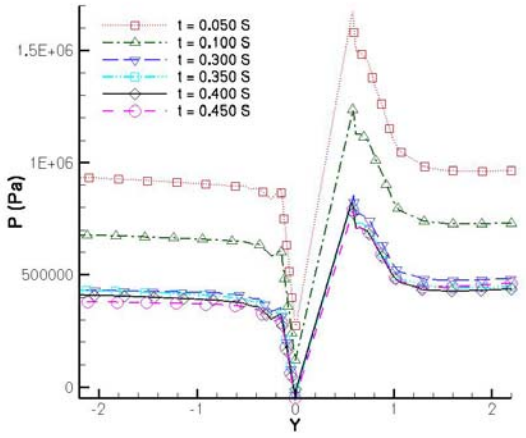

Figure 10. Pressure at line BB when the plate is spinning

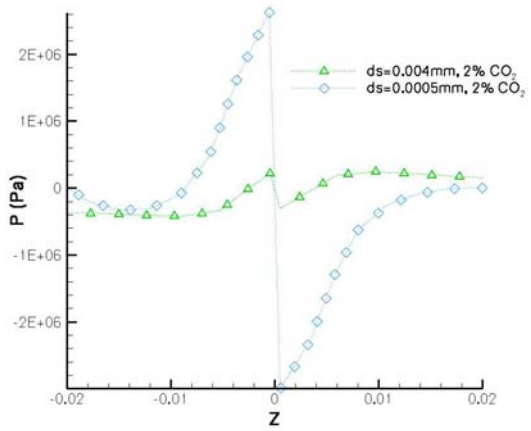

Figure 8. Pressure profile along line AA as in Figure 6; the effect of the distance of the clay and the bubble

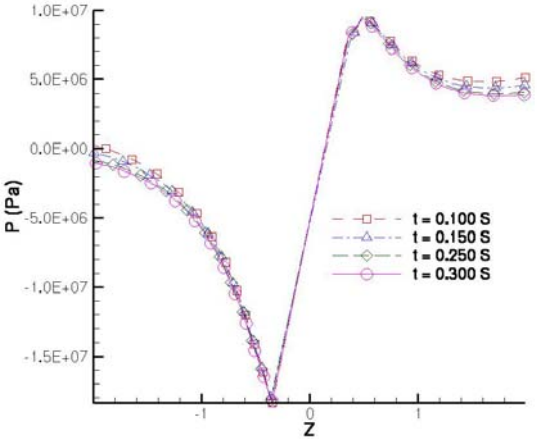

Figure 11. Pressure profile along line through the top and bottom of the squeezed sphere

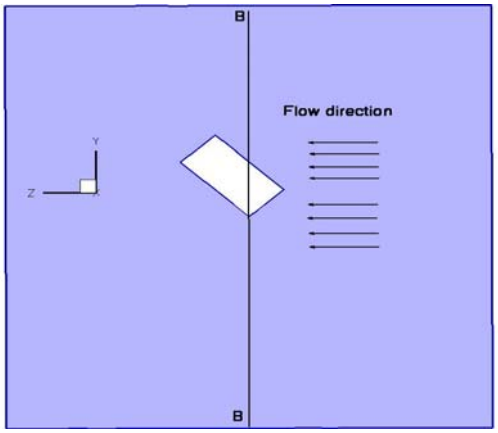

Figure 9. Solid plate in shear flow